Magnetic Resonance Electrical Impedance Tomography (MREIT): Simulation Study of J-Substitution Algorithm

Ohin Kwon, Eung Je Woo*, *Member, IEEE*, Jeong-Rock Yoon, and Jin Keun Seo

***Abstract*—We developed a new image reconstruction algorithm for magnetic resonance electrical impedance tomography (MREIT). MREIT is a new EIT imaging technique integrated into magnetic resonance imaging (MRI) system. Based on the assumption that internal current density distribution is obtained using magnetic resonance imaging (MRI) technique, the new image reconstruction algorithm called J-substitution algorithm produces cross-sectional static images of resistivity (or conductivity) distributions. Computer simulations show that the spatial resolution of resistivity image is comparable to that of MRI. MREIT provides accurate high-resolution cross-sectional resistivity images making resistivity values of various human tissues available for many biomedical applications.**

***Index Terms*—Electrical impedance tomography, internal current density, MRI, MREIT.**

I. Introduction

In electrical impedance tomography (EIT), we try to reconstruct a cross-sectional resistivity (or conductivity) image of a subject using boundary voltage and current measurements. Since the 1980s, several static EIT image reconstruction algorithms have been published [1]–[4]. In static EIT imaging, the absolute values of a cross-sectional resistivity distribution are reconstructed. Static image reconstruction is a kind of inverse problem showing inherently severe ill-posed characteristics [2], [5]. There are two major problems in static EIT imaging. One is the modeling error in capturing the boundary shape of the subject for the construction of computer model. The other is the inherent low sensitivity of boundary measurements to any changes of internal tissue resistivity values. For these reasons, static EIT imaging is still far from clinical applications.

Lately, a new magnetic resonance imaging (MRI) technique has been developed for the measurements of the internal current density distribution [6]–[10]. While we inject current through electrodes attached on the boundary of a subject, MR images are obtained using a spin-echo sequence synchronized with current pulses. Since the injected current generates small magnetic field, these MR images include the effects of injection current as perturbation in the phase of images. Given MR images with phase perturbation, we can compute the magnitude of current density at each pixel of the MR image. Gamba and Delpy successfully measured the current density distribution in an intact piglet head using this technique [6]. Even though currently this requires rotating the subject within the main magnet, we believe that more practical and accurate method will be available soon.

We propose utilizing internal current density data to reconstruct static cross-sectional resistivity images. We call this new imaging method magnetic resonance electrical impedance tomography (MREIT). Since MR images of a subject are available, we can minimize the modeling error in boundary shape of the subject. Furthermore, the internal current density data eliminate the severe sensitivity problem in conventional EIT image reconstruction. The major disadvantage of MREIT is the requirement of the expensive MRI system. However, since MRI is becoming more common in modern clinical situation, the advantage of getting accurate high-resolution resistivity images will overcome the cost problem. Furthermore, MREIT will be a new enhancement in conventional MRI system providing both MR images and static resistivity images.

In 1994, a new EIT image reconstruction algorithm was proposed using internal current density distribution measured by MRI technique [11]. By adjusting resistivity distribution of a computer model of a subject, they tried to minimize the error between the measured current density from the subject and the computed current density of the model using the finite element method. However, the algorithm did not utilize the internal current density data effectively resulting in a poor spatial resolution and convergence characteristics. In this paper, we assume that internal current density distribution is available from an MRI system including added current injection capability. We propose a new static resistivity image reconstruction algorithm called J-substitution algorithm. Several results from computer simulations will show that accurate high-resolution static resistivity imaging with improved convergence characteristics is possible.

II. Methods

Reconstruction of resistivity image by MREIT begins with a numerically implementable relationship between the resistivity and the corresponding current density due to injection current.

Manuscript received November 15, 2000; revised March. 22, 2001. The work of O. Kwon was supported by the Faculty Research Fund of Konkuk University in 2001. The work of E. J. Woo was supported by Kyung Hee University and the KOSEF under Grant R01-2000-00385. The work of J. K. Seo was supported by the Korea Research Foundation under Grant 99-005-D0009. *Asterisk indicates corresponding author*.

O. Kwon is with the Department of Mathematics, Konkuk University, Seoul 143-701, Korea.

*E. J. Woo is with the School of Electronics and Information, Kyung Hee University, Kyungki 449-701, Korea (e-mail: ejwoo@khu.ac.kr).

J. R. Yoon is with the School of Mathematics, Korea Institute for Advanced Study, Seoul 130-012, Korea.

J. K. Seo is with the Department of Mathematics, Yonsei University, Seoul 120-749, Korea

Publisher Item Identifier S 0018-9294(02)00647-X.

In the present form of the J-substitution algorithm, we use only the magnitude of the current density. Later in this paper, we will discuss the reason why we use only the magnitude. Let Ω denote two-dimensional cross section of an electrically conducting body with positive resistivity distribution denoted by ρ^*. The resistivity distribution ρ^* in the region Ω and the voltage V_{ρ^*} are unknown but the magnitude of the current density $J^* = |\boldsymbol{J}^*|$ is given by MRI technique with injection currents I through electrodes attached on the boundary $\partial\Omega$. These currents I produce current densities on the boundary whose inward pointing normal component is denoted by j_I, so that the compatibility condition $\int_{\partial\Omega} j_I\, ds = 0$ is satisfied. The inverse problem is to reconstruct ρ^* from the known data I, J^* and physical laws of electromagnetics.

A. Problem Definition

We construct a mathematical model of the body Ω with the same geometrical shape. For any given resistivity ρ of the model, the corresponding voltage V_ρ satisfies the boundary value problem

$$\nabla \cdot \left(\frac{1}{\rho}\nabla V_\rho\right) = 0 \quad \text{in } \Omega \tag{1}$$

with the boundary condition

$$\frac{1}{\rho}\frac{\partial V_\rho}{\partial n} = j_I \quad \text{on } \partial\Omega \tag{2}$$

where j_I is the current density at the boundary $\partial\Omega$ and n denotes the unit outward normal vector at the boundary $\partial\Omega$. It is well known that ∇V_ρ is uniquely determined by the resistivity ρ and the boundary current density j_I induced by I [12]. Here, I is identical to the injection current we used for the measurement of J^*.

For the case of $\rho = \rho^*$, our inverse problem is reduced to the following nonlinear boundary value problem:

$$\begin{aligned} \nabla \cdot \left(\frac{J^*}{|\nabla V_{\rho^*}|}\nabla V_{\rho^*}\right) &= 0 \quad \text{in } \Omega \\ \frac{J^*}{|\nabla V_{\rho^*}|}\frac{\partial V_{\rho^*}}{\partial n} &= j_I \quad \text{on } \partial\Omega \end{aligned} \tag{3}$$

where $1/\rho^*$ in (1) and (2) is substituted by $J^*/|\nabla V_{\rho^*}|$ since $\boldsymbol{J}^* = -1/\rho^* \nabla V_{\rho^*}$. Imaging resistivity ρ^* means to find a constructive map $\{I, J^*\} \longrightarrow \rho^*$ from the above highly nonlinear equation. Due to this intricate relation, it is almost impossible to find an explicit expression of ρ^* in terms of J^* and I. So, we develop an iterative scheme to search for the true solution ρ^*.

B. Image Reconstruction Algorithm: J-Substitution Algorithm

Related to the boundary value problem in (1) and (2), we introduce the following cost functional $\Psi(\rho)$:

$$\Psi(\rho) := \int_\Omega \left| J^*(\mathbf{r}) - \frac{1}{\rho(\mathbf{r})}E_\rho(\mathbf{r})\right|^2 d\mathbf{r} \tag{4}$$

where $J^*(\mathbf{r})$ is the magnitude of the observed interior current density and $E_\rho(\mathbf{r}) := |\nabla V_\rho(\mathbf{r})|$ is the magnitude of the calculated electric field intensity obtained by solving (1) and (2) for a given ρ. After discretization of the model $\bar{\Omega} = \cup_{k=0}^{N-1}\bar{\Omega}_k$ with the same area for all Ω_k, we get the following squared residual sum R:

$$R(\sigma_0, \ldots, \sigma_{N-1}) := \sum_{k=0}^{N-1}\int_{\Omega_k} |J^*(\mathbf{r}) - \sigma_k E_\rho(\mathbf{r})|^2 d\mathbf{r} \tag{5}$$

where Ω_k is the kth element of the model, σ_k is the reciprocal of the resistivity on Ω_k that is assumed to be a constant on each element. Note that in this case, the resistivity distribution is expressed by $\rho(\mathbf{r}) = \sum_{k=0}^{N-1}(1/\sigma_k)\chi_{\Omega_k}(\mathbf{r})$, where $\chi_{\Omega_k}(\mathbf{r})$ denotes the indicator function of Ω_k, hence, the electric field intensity $E_\rho(\mathbf{r})$ in (5) is also a function of $(\sigma_0, \ldots, \sigma_{N-1})$. To update the resistivity from the zero gradient argument for the minimization of the squared residual sum, we differentiate (5) with respect to σ_m for $m = 0, \ldots, N-1$ to get

$$\begin{aligned} 0 = \frac{\partial R}{\partial \sigma_m} &= 2\int_{\Omega_m} E_\rho(\mathbf{r})(\sigma_m E_\rho(\mathbf{r}) - J^*(\mathbf{r}))\, d\mathbf{r} \\ &\quad + 2\sum_{k=0}^{N-1}\int_{\Omega_k} \sigma_k \frac{\partial E_\rho(\mathbf{r})}{\partial \sigma_m}(\sigma_k E_\rho(\mathbf{r}) - J^*(\mathbf{r}))\, d\mathbf{r}. \end{aligned} \tag{6}$$

This leads to the following approximate identity:

$$\begin{aligned} 0 \approx\ & E_\rho(\mathbf{r}_m)(\sigma_m E_\rho(\mathbf{r}_m) - J^*(\mathbf{r}_m)) \\ & + \sum_{k=0}^{N-1}\sigma_k \frac{\partial E_\rho(\mathbf{r}_k)}{\partial \sigma_m}(\sigma_k E_\rho(\mathbf{r}_k) - J^*(\mathbf{r}_k)) \end{aligned} \tag{7}$$

for $m = 0, \ldots, N-1$, where $\mathbf{r}_k$ is the center point of the element Ω_k and we used the simplest quadrature rule. Hence, we obtain the following updating strategy to minimize the residual sum in (5):

$$\frac{1}{\bar{\rho}_m} = \bar{\sigma}_m := \frac{J^*(\mathbf{r}_m)}{E_\rho(\mathbf{r}_m)} \quad \text{for } m = 0, \ldots, N-1 \tag{8}$$

where $\bar{\rho}_m$ is a new resistivity value on Ω_m and $E_\rho(\mathbf{r}_m)$ is the calculated electric field intensity at the center point of Ω_m from an old resistivity distribution $\rho(\mathbf{r}) = \sum_{k=0}^{N-1}(1/\sigma_k)\chi_{\Omega_k}(\mathbf{r})$.

Before developing an algorithm, it is necessary to check if the data pair $\{I, J^*\}$ has sufficient information to determine ρ^*. Unfortunately, it is possible that two different resistivity distributions may correspond to the same pair $\{I, J^*\}$.

Let us consider a conducting material consisting of two media with different resistivities. It is well known that the normal component of $\boldsymbol{J}$ is continuous across the interface while its tangential component changes. Thus, the magnitude of the current density will change if the tangential components of $\boldsymbol{J}$ at the interface is nonzero. Hence, J plays an important role to reconstruct resistivity image due to its change when current crosses an interface nonorthogonally between two media. However, J may not provide any information for imaging a portion of the interface where current flows orthogonally. In order to clearly illustrate this, we consider the following counter example:

$$\Omega = (0,2)\times(0,1), \quad J = 1 \text{ in } \Omega$$

$$j_I(x,y) = \begin{cases} -1, & \text{for } x = 0, 0 < y < 1 \\ 1, & \text{for } x = 2, 0 < y < 1 \\ 0, & \text{otherwise} \end{cases}$$

where we denote the coordinates of the position vector $\mathbf{r}$ as $(x, y) \in \mathbb{R}^2$. Then there are infinitely many solutions for all a and k satisfying $0 < a < a + k/(k-1) < 2$

$$\rho_{a,k}(x,y) = \begin{cases} k, & \text{if } 0 < x < a \\ 1, & \text{if } a < x < a + k/(k-1) \\ k, & \text{if } a + k/(k-1) < x < 2. \end{cases}$$

The corresponding voltage to $\rho_{a,k}$ given by

$$V_{k,a}(x,y) = \begin{cases} x, & \text{if } 0 < x < a \\ (x + (k-1)a)/k, & \text{if } a < x < a + k/(k-1) \\ x - 1, & \text{if } a + k/(k-1) < x < 2 \end{cases}$$

is a solution of the problem in (1) and (2). This undesirable nonuniqueness could happen when $\boldsymbol{J}$ is orthogonal to the level curve of the resistivity ρ. In such a case, $\boldsymbol{J}(\mathbf{r})$ does not contain any information on the variation of $\rho(\mathbf{r})$. For this reason, we will apply two currents, I^1 and I^2 in order that the corresponding two current densities satisfy

$$|\boldsymbol{J}^1 \times \boldsymbol{J}^2| \neq 0. \tag{9}$$

For this purpose, in our MREIT system four electrodes are placed at four sides (east, south, west, north) on the boundary so that we can apply two different current flows using two pairs of electrodes. Let I^1 and I^2 be the two currents from two pairs of electrodes. Two sets of current density data, $J^1 = |\boldsymbol{J}^1|$ and $J^2 = |\boldsymbol{J}^2|$ induced by I^1 and I^2, respectively, can now be used to image the resistivity distribution. Due to the position of electrodes, two vectors $\boldsymbol{J}^1$ and $\boldsymbol{J}^2$ are not in the same (or opposite) direction and, thus, satisfy (9). This is proved for any resistivity distributions that we can encounter in medical applications [13]. Therefore, at least one of J^1 and J^2 changes abruptly at the interface of two media where any change of resistivity occurs.

Our inverse problem is to determine ρ^* from two pairs of data $(I^q, J^q), q = 1, 2$ and our goal is to develop a reconstruction algorithm for ρ^*. The reconstruction algorithm called J-substitution algorithm for this nonlinear problem in (3) is as follows.

1) *Initial guess*: For the initial guess, we may choose a homogeneous resistivity ρ^0, for example, $\rho^0 := 1$.
2) *Forward solver*: For given resistivity $\rho^{2p+q} (q = 1, 2$ and $p = 0, 1, 2, \ldots)$, we solve the forward problem given by

$$\nabla \cdot \left(\frac{1}{\rho^{2p+q}} \nabla V_p^q \right) = 0 \quad \text{in } \Omega$$
$$\frac{1}{\rho^{2p+q}} \frac{\partial V_p^q}{\partial n} = j_{I^q} \quad \text{on } \partial\Omega \quad \text{and} \quad \int_{\partial\Omega} V_p^q ds = 0. \tag{10}$$

   Finite element method or finite difference method is commonly used to solve the forward problem in (10). In this paper, we use the cell-centered finite difference method which is one of the popular numerical methods [14].
3) Update ρ^{2p+q+1} as follows:

$$\rho^{2p+q+1} := \frac{|\nabla V_p^q|}{J^q}. \tag{11}$$

   Now let us consider two resistivity distributions ρ and $\rho_\alpha := \alpha\rho$ with a positive constant α for the same subject Ω. If we inject the same current pattern, the induced internal current density J corresponding to ρ is identical to J_α corresponding to ρ_α. However, the corresponding voltages satisfy $V_\alpha = \alpha V$. Therefore in order to reconstruct the absolute resistivity distribution, the updating strategy in (11) should be modified as

$$\rho^{2p+q+1} := \frac{|\nabla V_p^q|}{J^q} \frac{f_{\rho^*}^q}{f_{\rho^{2p+q}}^q} \tag{12}$$

   where $f_{\rho^*}^q$ is the measured voltage difference between two current injection electrodes for the injection current I^q and $f_{\rho^{2p+q}}^q$ is the corresponding voltage difference when the resistivity distribution is given by ρ^{2p+q}.
4) If $|\rho^{2p+q+1} - \rho^{2p+q}| < \epsilon$ for some measurement precision ϵ, stop; otherwise go back to Step 2) with $q = q+1$ when $q = 1$ or $p = p+1$ and $q = 1$ when $q = 2$.

C. Forward Solver

For the target region Ω, we choose the square region $(-1, 1) \times (-1, 1)$ only for simplicity. Since our algorithm is to determine $N \times N$ resistivity values which exactly correspond to MR image, we divide Ω uniformly into $N \times N$ axis-parallel subsquares Ω_{i+jN} with the center point (x_i, y_j) where $i = 0, \ldots, N-1$ and $j = 0, \ldots, N-1$. Let h denote the side length of each subsquare Ω_k. We assume that the voltage at the center point (x_i, y_j) of the cell Ω_{i+jN} is approximated by

$$v_{i+jN} := V_\rho(x_i, y_j). \tag{13}$$

In our cell-centered finite difference method, we assume the resistivity ρ is constant on each subsquare Ω_k, say ρ_k. In order to explain the cell-centered method clearly, note that there are three kinds of subsquares, that is, the interior cells, boundary cells, and corner cells.

First, let us take our attention to one fixed element Ω_k which lies in the interior of Ω, that is

$$k = i + jN, \quad 1 \leq i, \quad j \leq N-2.$$

Since $\nabla \cdot ((1/\rho_k)\nabla V_\rho) = 0$ on each square element Ω_k, integrating by parts we get

$$0 = \frac{1}{\rho_k} \int_{\Omega_k} \nabla \cdot (\nabla V_\rho)\, d\mathbf{r} = \frac{1}{\rho_k} \int_{\partial\Omega_k} \frac{\partial V_\rho}{\partial n} ds. \tag{14}$$

On the other hand, using the simplest quadrature rule we obtain the following approximation:

$$\begin{aligned} &\frac{1}{\rho_k} \int_{\partial\Omega_k} \frac{\partial V_\rho}{\partial n} ds \\ &\approx \frac{h}{\rho_k} \left\{ \partial_x V_\rho \left(\frac{x_i + x_{i+1}}{2}, y_j \right) - \partial_x V_\rho \left(\frac{x_i + x_{i-1}}{2}, y_j \right) \right. \\ &\qquad \left. + \partial_y V_\rho \left(x_i, \frac{y_j + y_{j+1}}{2} \right) - \partial_y V_\rho \left(x_i, \frac{y_j + y_{j-1}}{2} \right) \right\}. \end{aligned} \tag{15}$$

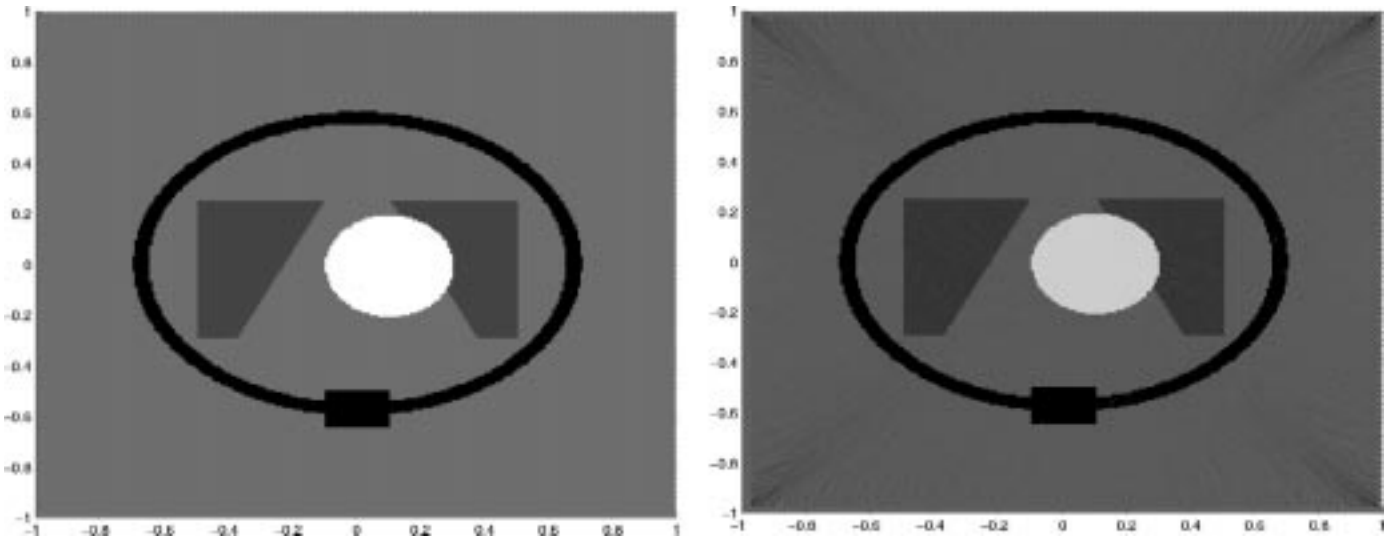

(a) (b)

Fig. 1. (a) Target resistivity distribution of Toy model. (b) Reconstructed image after 20 iterations with ±5% noise.

Four terms in (15) are values of the normal derivative of V_ρ at the midpoints of four sides of the element Ω_k. Since we can calculate all of these terms in the same way, we describe how to compute the third term. The interface condition between two elements Ω_k and Ω_{k+N} can be understood approximately as

$$\frac{V_\rho\left(x_i, \frac{y_j+y_{j+1}}{2}\right) - v_k}{\rho_k} \approx \frac{v_{k+N} - V_\rho\left(x_i, \frac{y_j+y_{j+1}}{2}\right)}{\rho_{k+N}} \quad (16)$$

which gives

$$V_\rho\left(x_i, \frac{y_j+y_{j+1}}{2}\right) = \frac{\sigma_{k+N}v_{k+N} + \sigma_k v_k}{\sigma_{k+N}+\sigma_k}. \quad (17)$$

Denoting

$$a_{k,k\pm N} = \frac{\sigma_k\sigma_{k\pm N}}{\sigma_k+\sigma_{k\pm N}} \quad \text{and} \quad a_{k,k\pm 1} = \frac{\sigma_k\sigma_{k\pm 1}}{\sigma_k+\sigma_{k\pm 1}}, \quad (18)$$

the third term in (15) is approximated as

$$h\sigma_k\partial_y V_\rho\left(x_i, \frac{y_j+y_{j+1}}{2}\right) \approx 2a_{k,k+N}(v_{k+N}-v_k). \quad (19)$$

Repeating the same calculation for the other three terms in (15), we get

$$0 = a_{k,k+N}v_{k+N} + a_{k,k-N}v_{k-N} + a_{k,k+1}v_{k+1} + a_{k,k-1}v_{k-1} - a_{k,k}v_k \quad (20)$$

where $a_{k,k} = \{a_{k,k+N} + a_{k,k-N} + a_{k,k+1} + a_{k,k-1}\}$.

Second, let us consider one fixed element Ω_k which is on the boundary $\partial\Omega$. For example, we consider an element adjacent to the left boundary, that is

$$k = i + jN \quad \text{for } i = 0 \text{ and } 1 \le j \le N-2.$$

Analogous arguments as above yield

$$I(-1, y_k) = a_{k,k+N}v_{k+N} + a_{k,k-N}v_{k-N} + a_{k,k+1}v_{k+1} - a_{k,k}v_k \quad (21)$$

where $a_{k,k} = \{a_{k,k+N} + a_{k,k-N} + a_{k,k+1}\}$ and

$$I(-1, y_k) = \int_{\partial\Omega_k\cap\partial\Omega} j_I ds.$$

Third, for the four corner elements Ω_k, we have

$$k = i + jN \quad \text{for } i, j = 0 \text{ or } N-1.$$

When we consider the left lower corner element, similar arguments yield

$$I(-1, y_0) + I(x_0, -1) = a_{k,k+N}v_{k+N} + a_{k,k+1}v_{k+1} - a_{k,k}v_k \quad (22)$$

where $a_{k,k} = \{a_{k,k+N} + a_{k,k+1}\}$ and

$$I(-1, y_0) + I(x_0, -1) = \int_{\partial\Omega_k\cap\partial\Omega} j_I ds.$$

From (20)–(22), we can construct the following linear system:

$$A\mathbf{x} = \mathbf{b} \quad (23)$$

where A is $N^2 \times N^2$ matrix, $\mathbf{x} = (v_0, v_1, \ldots, v_{N^2-1})$, and $\mathbf{b}$ is the injection current vector associated with I.

However the master matrix A is singular, so we cannot directly solve the linear system. Since the solution space of the system is one dimensional, we set $v_0 = 0$ and modify the matrix A to the new matrix by changing only the first row of A in such a way that $b_0 = 0, a_{0,0} = 1$, and $a_{0,k} = 0$ for all $k = 1, \ldots, N^2-1$. We use the conjugate gradient method in solving the linear system in (23).

III. Results

A. Toy Model

Fig. 1(a) shows a target model called Toy model with 256×256 pixels ($N = 256$). It consists of four anomalies with different resistivity values. The relative resistivities with

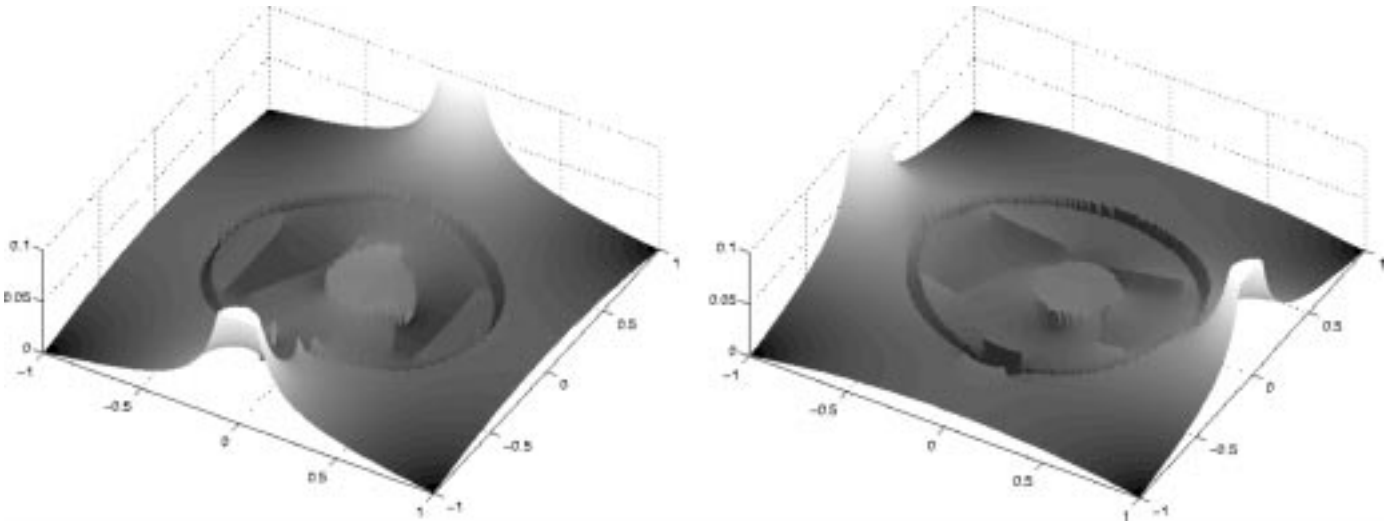

(a) (b)

Fig. 2. Simulated current density measurements with ±5% noise. (a) J^1 of Toy model. (b) J^2 of Toy model.

respect to the background are 0.25 in the white disk, 2.0 in two grey trapezoids, and 5.0 in the dark ring. J^1 and J^2 in Fig. 2(a) and (b) are simulated current density measurements with ±5% random noise in the following sense:

$$J^i(\mathbf{r}_k) = J^i_{\text{true}}(\mathbf{r}_k) + ||J^i_{\text{true}}|| \times rand\_num \times nos\_lev \quad (24)$$

for $i = 1, 2$ and $k = 0, \ldots, N^2 - 1$, where $||J^i_{\text{true}}||$ is the L^2-norm in $\Omega = (-1, 1) \times (-1, 1)$ of the noiseless simulated current density measurements, *rand_num* denotes a random number distributed in $(-1, 1)$, and *nos_lev* is 0.05 for ±5% random noise level.

After 20 iterations with the homogeneous initial guess, we obtain the reconstructed resistivity image shown in Fig. 1(b). At the second iteration step, the intermediate image already shows correct boundaries of anomalies, and then the resistivity values within each anomaly approach the true ones in the subsequent iterations. The early appearance of anomaly stems from the discontinuous nature of current density at the boundary and implies that J-substitution algorithm is highly accurate in describing the boundary. This feature will be desirable in reconstructing the shapes of organs or clusters of tissues with different resistivity values.

The convergence characteristics of the algorithm is studied in terms of the relative L^2-error defined as

$$E_p := \frac{||\rho^* - \rho^p||}{||\rho^*||} \quad (25)$$

where ρ^p denotes the resistivity distribution at pth iteration and ρ^* is the target resistivity distribution. The convergence behavior in Fig. 3(a) with random noise of ±5%, ±2.5%, and 0% shows that J-substitution algorithm is quite stable to noisy data. Other static EIT image reconstruction algorithms using nonlinear optimization techniques tend to amplify measurement errors in the reconstructed image due to the ill-posedness of the problem. J-substitution algorithm alleviates this difficulty by effectively utilizing the internal current density information. Since it is highly possible for the current density measurements to contain a large amount of noise, this noise endurance is a strong merit of our algorithm.

In Fig. 3(a), we start with the homogeneous initial guess using the same resistivity value as in the background of the target. In MREIT, we can utilize *a priori* structural information from MR images in choosing a better initial guess. For example, we choose the resistivity value of 0.2 in the white disk, 1.5 in two gray trapezoids, and 3.0 in the dark ring to produce a preconditioned initial guess. Fig. 3(b) shows that the convergence behavior is significantly improved compared with the homogeneous initial guess when we use this preconditioned initial guess. Fig. 3(c) and (d) shows how resistivity values of three anomalies are converged to the true values with different initial guesses. In simulations for Fig. 3(b)-(d), we use the current density data contaminated with ±5% noise.

B. Realistic Model

The second model is introduced in order to show the feasibility of J-substitution algorithm in a very complicated realistic case. Because a real resistivity distribution of the human body is not available, we bravely imagine that the resistivity of each pixel is proportional to the pixel value of a CT image. Fig. 4(a) shows a realistic target model with 256×256 pixels. Fig. 5(a) and (b) shows J^1 and J^2 which are simulated current density measurements with ±5% random noise. The reconstructed resistivity image using the homogeneous initial guess is shown in Fig. 4(b) after 40 iterations. Fig. 6 shows the convergence characteristics and the minimum relative error is 0.237 11 with ±5% random noise.

IV. Discussion

MREIT solves many technical problems in conventional EIT. In static EIT imaging, we usually use 32 or more electrodes to achieve 5% spatial resolution at most. MREIT requires at least four electrodes which is fewer than needed in EIT. This avoids the cumbersome electrode attachment procedure in EIT.

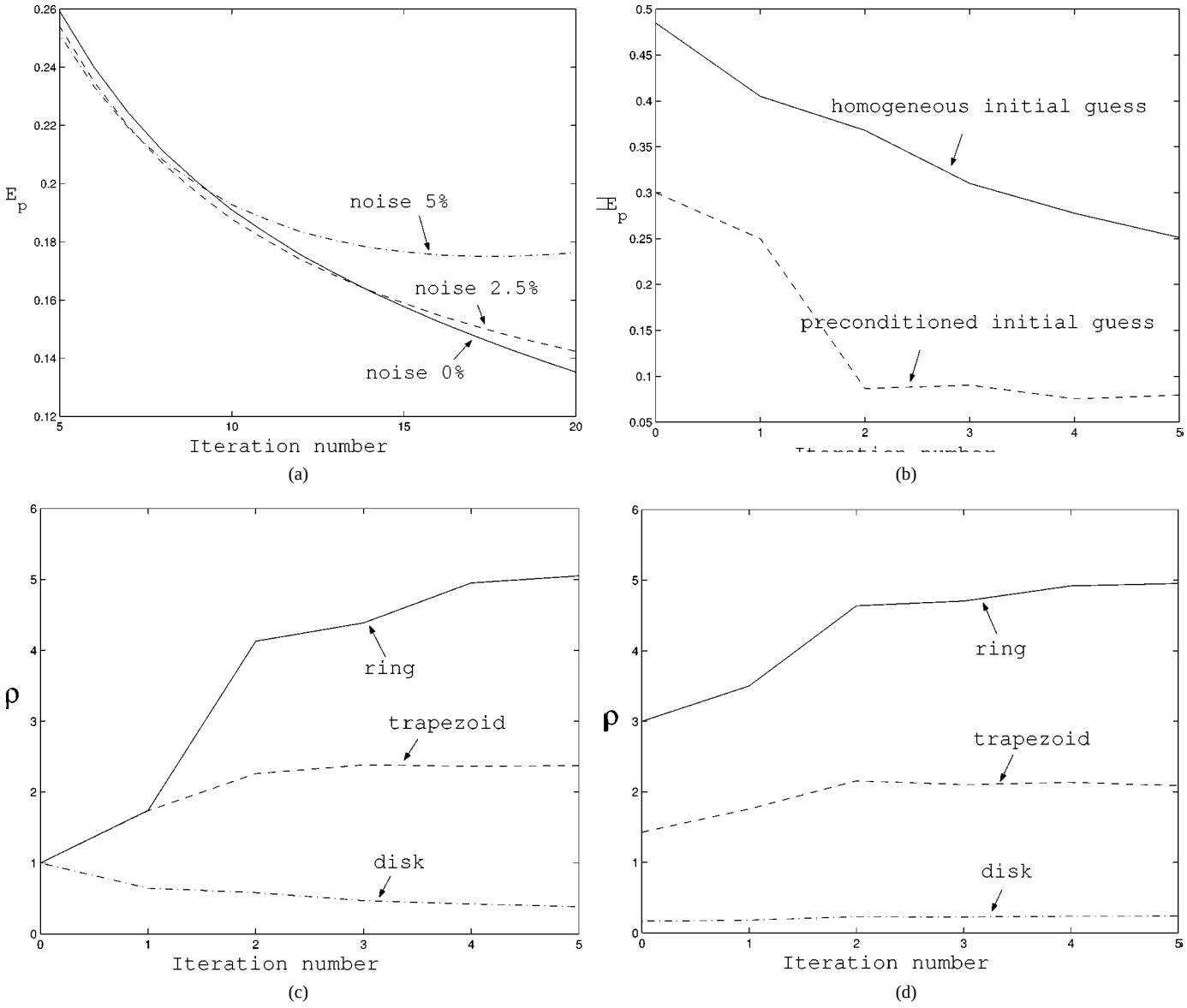

Fig. 3. (a) Convergence characteristics (from fifth through twentieth iteration) of J-substitution algorithm for Toy model with different noise levels. (b) Convergence characteristics (from first through twentieth iteration) of J-substitution algorithm for Toy model with different initial guesses. (c) Resistivities of anomalies approach true values with a homogeneous initial guess as we increase the number of iterations. (d) Resistivities of anomalies approach true values with a preconditioned initial guess as we increase the number of iterations.

In MREIT, we can easily obtain the boundary shape of the subject since MR images are available. This eliminates the problem related with modeling error. The severe sensitivity problem inherent in EIT is removed by utilizing internal current density data. MREIT takes the advantage of MRI as structural imaging modality and provides accurate tissue resistivity images that no other medical imaging modality can do.

In this paper, we used only the magnitude of the current density vector for the following reasons. When two pairs of electrodes are used as discussed in our paper, the magnitude information is sufficient to guarantee the uniqueness of the reconstructed resistivity image. This is proved under the assumption of piecewise constant resistivity distribution [13]. Thus, for noise-free current density data, the reconstructed image using only the magnitude must be the same as the image using the direction as well. We will study the noise characteristics of the current density measurements and expand the algorithm to include the direction as well if it is helpful. However, we speculate that using only the magnitude information would be enough against noisy current density measurements.

Based on the simulation studies described in this paper, our algorithm shows convergence characteristics good enough for most highly complicated resistivity distributions that we can face in medical applications. We also observed that any reasonable initial guesses make the algorithm convergent to the degree needed for successful image reconstructions. As a part of our future works, we will rigorously study the mathematical analysis of the convergence.

J-substitution algorithm described in this paper does not require nonlinear least squares optimization such as Newton-type algorithm which is computationally expensive. Since our algorithm requires simple substitutions as shown in (12), it only needs a fast forward solver for the solution of (23). We may use the multigrid method for cell-centered finite difference scheme

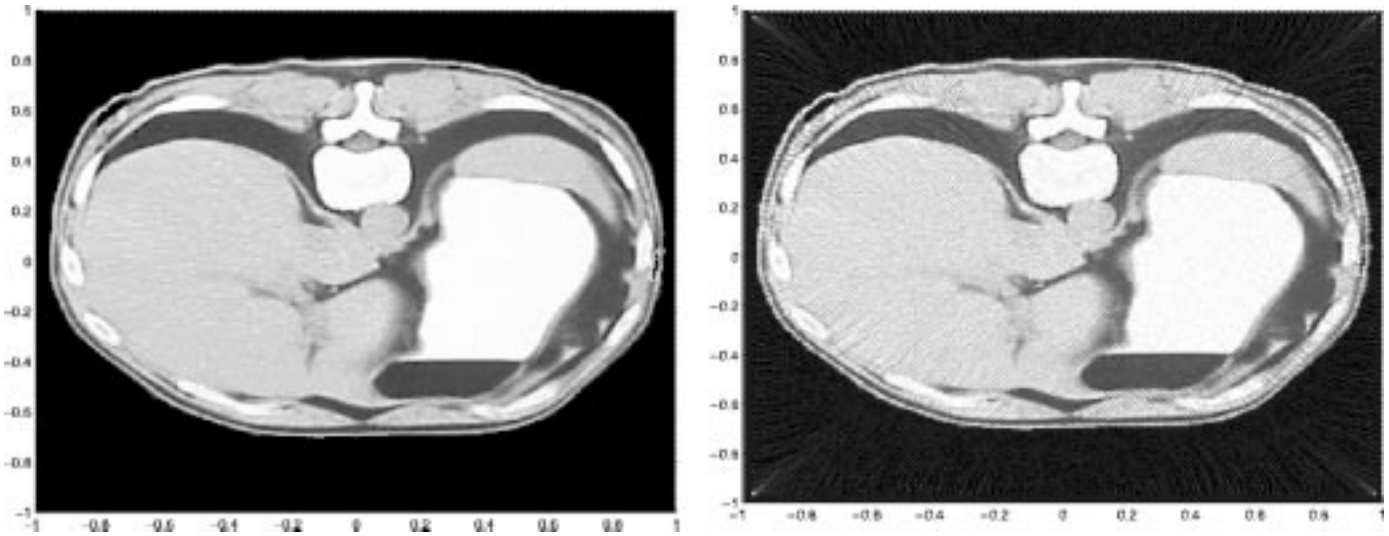

(a) (b)

Fig. 4. (a) Target resistivity distribution of realistic model. (b) Reconstructed image after 40 iterations with $\pm 5\%$ noise.

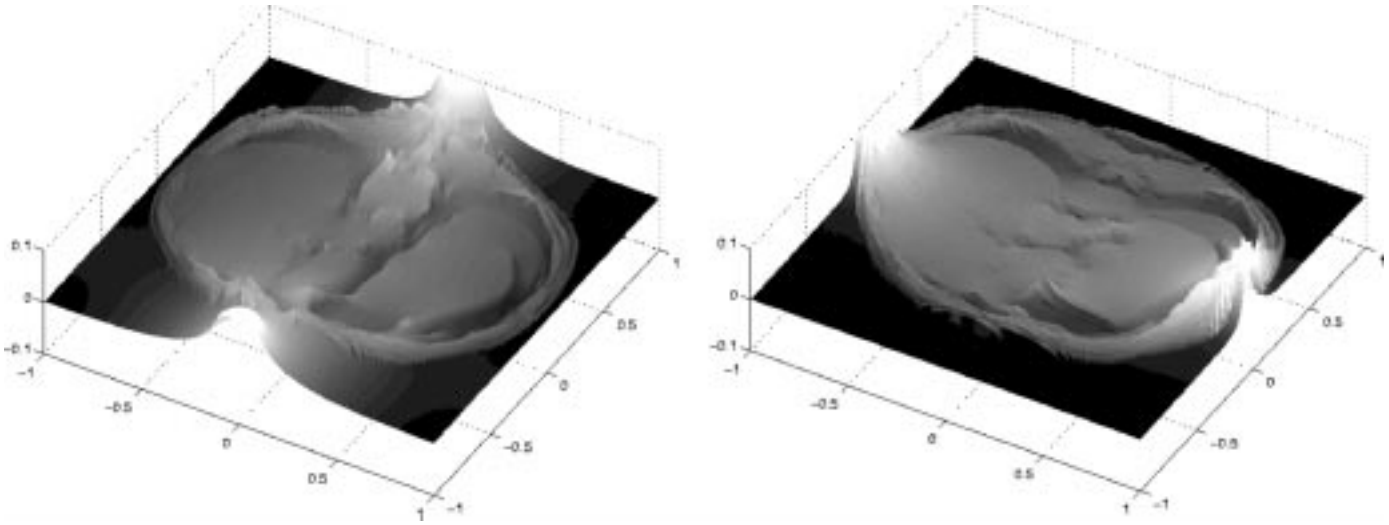

(a) (b)

Fig. 5. Simulated current density measurements with $\pm 5\%$ noise. (a) J^1 of realistic model. (b) J^2 of realistic model.

or finite element method with sparse matrix techniques to accommodate any irregular boundary. In our future works, we will investigate the possibilities of improvement to seek for the ultimate performance of J-substitution algorithm.

We can construct an MREIT system by adding a constant current source, switching circuit, and at least four electrodes to any conventional MRI system. We are constructing a prototype of MREIT system based on 0.3 T laboratory MRI system with bore diameter of 25 cm. We construct a phantom with different resistivity values that we can rotate in the magnet for measuring internal current density data. We expect the major problem in MREIT is the accuracy in the measured current density. Future studies will include the optimal MR imaging technique for accurate measurements of internal current density. We also need to study three-dimensional MREIT image reconstruction.

V. Conclusion

We proposed a new imaging technique, MREIT using J-substitution algorithm. Given reliable internal current density measurement techniques, MREIT can provide clinically useful cross-sectional resistivity images of a subject. Even though it requires an expensive MRI system, it solves many technical problems in conventional static EIT imaging. Computer simulations show that MREIT produces high resolution resistivity images. With future improvements in the construction of MREIT system including hardware and software, it will visualize totally new physiological information of resistivity distribution that no other imaging modality can provide. Accurate tissue resistivity values will be valuable in many biomedical application areas, especially where electric energy is utilized for diagnosis and treatment.

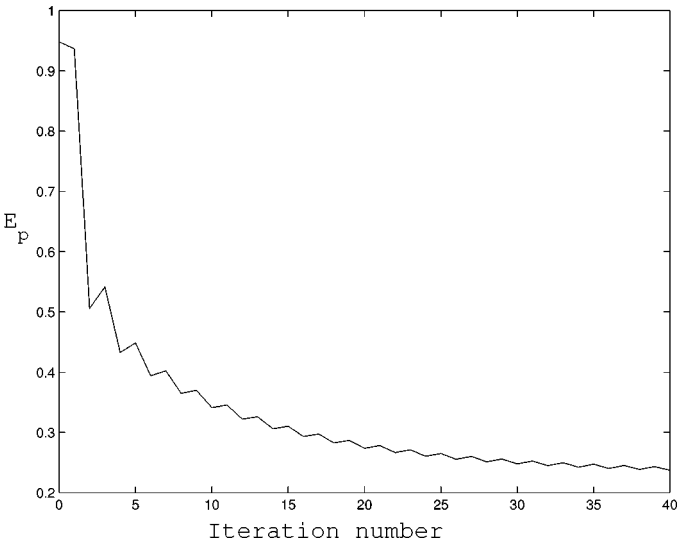

Fig. 6. Convergence characteristic of J-substitution algorithm for realistic model.

ACKNOWLEDGMENT

J. R. Yoon would like to acknowledge the helpful discussions on cell-centered finite difference method with Joon-Sang Lee in Korea Advanced Institute of Science and Technology.

REFERENCES

[1] J. G. Webster, Ed., *Electrical Impedance Tomography*, Bristol, U.K.: Adam Hilger, 1990.

[2] K. Boone, D. Barber, and B. Brown, "Imaging with electricity: Report of the European concerted action on impedance tomography," *J. Med. Eng. Tech.*, vol. 21, no. 6, pp. 201–232, 1997.

[3] M. Cheney, D. Isaacson, J. C. Newell, S. Simske, and J. Goble, "NOSER: An algorithm for solving the inverse conductivity problem," *Int. J. Imag. Syst. Tech.*, vol. 2, pp. 66–75, 1990.

[4] P. Edic, D. Isaacson, G. Saulnier, H. Jain, and J. C. Newell, "An iterative Newton-Raphson method to solve the inverse conductivity problem," *IEEE Trans. Biomed. Eng.*, vol. 45, pp. 899–908, July 1998.

[5] E. J. Woo, P. Hua, J. G. Webster, and W. J. Tompkins, "A robust image reconstruction algorithm and its parallel implementation in electrical impedance tomography," *IEEE Trans. Med. Imag.*, vol. 12, pp. 137–146, Mar. 1993.

[6] H. R. Gamba and D. T. Delpy, "Measurement of electrical current density distribution within the tissues of the head by magnetic resonance imaging," *Med. Biol. Eng. Comput.*, vol. 36, pp. 165–170, 1998.

[7] G. C. Scott, M. L. G. Joy, R. L. Armstrong, and R. M. Henkelman, "Measurement of nonuniform current density by magnetic resonance," *IEEE Trans. Med. Imag.*, vol. 10, pp. 362–374, June 1991.

[8] ——, "Sensitivity of magnetic-resonance current density imaging," *J. Mag. Reson.*, vol. 97, pp. 235–254, 1992.

[9] ——, "Electromagnetic considerations for RF current density imaging," *IEEE Trans. Med. Imag.*, vol. 14, pp. 515–524, Sept. 1995.

[10] Y. Z. Ider and L. T. Muftuler, "Measurement of ac magnetic field distribution using magnetic resonance imaging," *IEEE Trans. Med. Imag.*, vol. 16, pp. 617–622, Oct. 1997.

[11] E. J. Woo, S. Y. Lee, and C. W. Mun, "Impedance tomography using internal current density distribution measured by nuclear magnetic resonance," *SPIE*, vol. 2299, pp. 377–385, 1994.

[12] D. Gilbarg and N. S. Trudinger, *Elliptic Partial Differential Equations of Second Order*. Berlin, Germany: Springer-Verlag, 1983.

[13] S. Kim, O. Kwon, J. K. Seo, and J. R. Yoon, "On a nonlinear partial differential equation arising in magnetic resonance electrical impedance tomography," SIAM J. Math. Analysis, submitted for publication.

[14] D. Y. Kwak, "V-cycle multigrid for cell-centered finite differences," *SIAM J. Sci. Comput.*, vol. 21, pp. 552–564, 1999.

Ohin Kwon received the B.S., M.S., and Ph.D. degrees in mathematics from Seoul National University, Seoul, Korea, in 1988, 1990, and 1999, respectively.

Currently, he is an Assistant Professor of Mathematics at Konkuk University, Seoul, Korea. His research interests include electrical impedance tomography, domain decomposition, parallel computing, and inverse problems.

Eung Je Woo (S'83–M'90) received the B.S. and M.S. degrees in electronics engineering from Seoul National University, Seoul, Korea, in 1983 and 1985, respectively, and the Ph.D. degree in electrical and computer engineering from the University of Wisconsin, Madison, in 1990.

From 1990 to 1999, he was on the faculty of the Department of Biomedical Engineering, Konkuk University, Korea. Currently, he is Professor of the School of Electronics and Information, Kyung Hee University, Korea. He teaches undergraduate and graduate courses on the topic of medical instrumentation. His research interests include electrical impedance tomography, magnetic resonance electrical impedance tomography, RF ablation, patient monitoring system, and biomedical signal processing.

He is a contributing author to *Tactile Sensors for Robotics and Medicine*, J. G. Webster, Ed. (New York: Wiley, 1988) and *Electrical Impedance Tomography*, J. G. Webster, Ed. (Bristol, U.K.: Adam Hilger, 1990). Dr. Woo is a member of Korea Society of Medical and Biological Engineering and Institute of Electronics Engineers of Korea.

Jeong-Rock Yoon received the B.S. degree with honors in mathematics from Seoul National University, Korea, in 1993, and the M.S. and the Ph.D. degrees in mathematics from Korea Advanced Institute of Science and Technology, in 1995 and 2001, respectively with his thesis *Inverse problems for reconstructive imaging of inhomogeneities inside the body: mathematical theory, numerical algorithms, and biomedical applications*.

Currently, he is a Research Fellow in mathematics at Korea Institute for Advanced Study. His research interests include partial differential equations, numerical analysis, and inverse problems both in the theoretical and applied sense.

Jin Keun Seo received the B.S. degree from Yonsei University, Seoul, Korea, in 1985 and the M.S. and Ph.D. degrees from the University of Minnesota, Minneapolis, in 1991.

He is currently an Associate Professor of Mathematics at Yonsei University, Seoul, Korea. His research interests include electrical impedance tomography, partial differential equations, inverse problems, mathematical modeling, harmonic analysis, and wavelet and image processing.